BOUND-FREE PAIR PRODUCTION IN LHC Pb-Pb OPERATION AT 6.37 Z TeV PER BEAM

J.M. Jowett[*], M. Schaumann[†], B. Auchmann, C. Bahamonde Castro, M. Kalliokoski,
A. Lechner, T. Mertens, C. Xu, CERN, Geneva, Switzerland

Abstract

In the 2015 Pb-Pb collision run of the LHC, the power of the secondary beams emitted from the interaction point by the bound-free pair production (BFPP) process reached new levels while the propensity of the bending magnets to quench increased with the magnetic field. This beam power is about 35 times greater than that contained in the luminosity debris and is focussed on a specific location. As long foreseen, orbit bumps were introduced in the dispersion suppressors around the highest luminosity experiments to mitigate the risk by displacing and spreading out these losses. The BFPP beams were used to induce a controlled quench of a dipole magnet, thus providing the first direct measurement of the steady state quench level and demonstrating the need for new collimators around the ALICE experiment to intercept these secondary beams.

INTRODUCTION

Ultraperipheral electromagnetic interactions of Pb nuclei at the LHC are responsible for copious lepton-pair production. Most of this is innocuous except for a tiny proportion of (single) bound-free pair production (BFPP1):

$$^{208}\text{Pb}^{82+} + ^{208}\text{Pb}^{82+} \longrightarrow ^{208}\text{Pb}^{82+} + ^{208}\text{Pb}^{81+} + e^+, \quad (1)$$
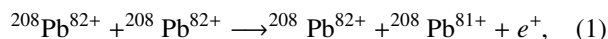
in which the electron is bound to one nucleus. As extensively discussed previously (see, eg, [1–6] and further references therein), the modified nuclei emerge from the collision point, as a narrow secondary beam with modified magnetic rigidity, following a dispersive trajectory (Figure 1) that impacts on the beam screen in a superconducting magnet in the dispersion suppressor (DS) downstream. These secondary beams emerge in both directions from every IP where ions collide and each carries a power $P_{\text{BFPP}} = L\sigma_{\text{BFPP}}E_b$ where L is the luminosity and $\sigma_{\text{BFPP}} \simeq 276$ b is the cross section at the 2015 run energy $E_b = 6.37Z$ TeV [7, 8]. These losses are much greater than the luminosity debris (generated by the nuclear collision cross-section of 8 b) and can quench magnets and directly limit luminosity.

ORBIT BUMP TECHNIQUE

During the 2015 Pb-Pb run [8] a peak $L = 3$–3.5×10^{27} cm^{-2}s^{-1} was achieved in IP1 and IP5. IP2 was levelled to the design value of $L = 1 \times 10^{27}$ cm^{-2}s^{-1}. Thus the BFPP1 beams emerging to the left and right of the ATLAS and CMS experiments, were carrying $P_{\text{BFPP}} \lesssim 80$ W. To reduce the risk of quenches, orbit

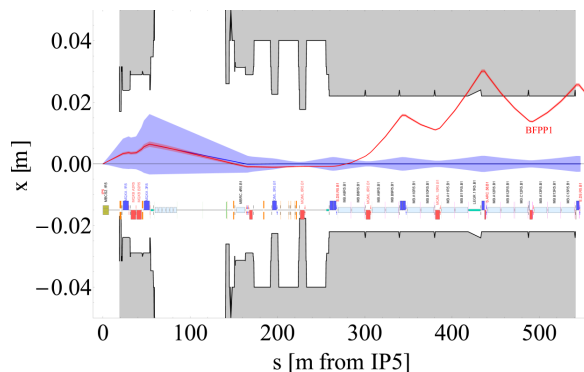---

[*] John.Jowett@cern.ch
[†] Michaela.Schaumann@cern.ch

Figure 1: Example of main (blue) and BFPP1 beam (red) radial envelopes, and aperture (grey), right of IP5 (at $s = 0$). Beamline elements are indicated schematically.

bumps around the impact locations were implemented in order to move the losses out of the dipole and into the connection cryostat ("missing dipole" in DS). Although the cryostat does not contain a coil, it still accommodates the superconducting bus bars. However, these bus bars have a higher quench level than coils and are located above the vacuum chamber where the Pb losses are ineffectual [9]. The green trajectory in Fig. 2 shows the new path of the BFPP ions modified by an orbit bump with a maximum amplitude of -3 mm around the quadrupole in cell 11 (Q11). These orbit bumps were used routinely and no luminosity production fill was interrupted by a quench.
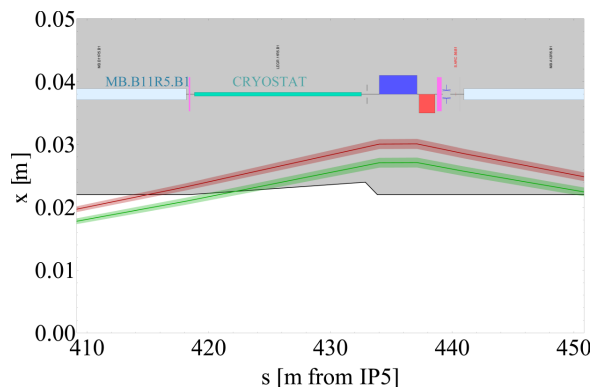

Figure 2: Zoom into Fig. 1 at the impact location of the BFPP beam. Red trajectory calculated without orbit bump, green with a bump amplitude of -3 mm at Q11.

BFPP QUENCH TEST

At the outset, it was thought unlikely that the available luminosity was enough to induce a magnet to quench but

there is a large uncertainty on the knowledge of the necessary power deposition. The BFPP beams can provide a very clean loss scenario that can be reconstructed with FLUKA [10,11] simulations that can then be used to improve the knowledge of the steady-state quench limit. Using the BFPP1 beam to induce a quench has the advantage that the impact point in the magnet can be controlled by modifying the orbit bumps, so that quenches at the end of the magnet, which would return less accurate estimates for the quench limits due to the specifics of the magnet design, can be avoided. Furthermore, the power in the BFPP beam is directly dependent on the luminosity, which can also be controlled with the beam separation at the IP.

Setup of the Experiment

The experiment was performed on 8 Dec 2015, with the highest available intensity and lowest transverse emittances available to that date to maximise the likelihood of a quench. The beams were prepared as for a standard physics fill up to the point of being put in collision. The average beam parameters at that point are listed in Table 1.

Table 1: Average Beam Parameters in the Experiment. Emittances $\varepsilon_{n(x,y)}$ are normalised values.

Fill number	4707
Ions per bunch N_b	$(1.9 \pm 0.3) \times 10^8$
Bunches colliding in IP5 k_{c5}	418
Bunch length σ_z	9.2 ± 0.3 cm
$\varepsilon_{n(x,y)}$ (Beam 1)	$(2.2, 1.2) \pm 0.2 \, \mu m$
$\varepsilon_{n(x,y)}$ (Beam 2)	$(2.0, 1.7) \pm 0.2 \, \mu m$

The loss location left of IP5 was chosen as most propitious for the experiment as it had the highest losses in the preceding fills and the beam impact point lay further inside the dipole in the absence of the orbit bump. At the other loss locations, the beams would impact closer to the end of the dipole or in the interconnect without orbit bump.

Further details of the procedure are given in [12].

Conducting the Experiment

Once the beams were colliding, they were re-separated in all IPs in order to reduce burn-off and husband peak luminosity for the experiment. The vertical separation at IP5 was reduced sufficiently to determine the impact point of the BFPP beam in the bending magnet based on the comparison of BLM signals and FLUKA simulations. From here the BFPP orbit bumps left of IP5 were reduced through zero and slightly inverted, until it was clear that the loss location had moved into the body of the dipole magnet.

Figure 3 shows the initial loss situation to the left side of IP5: in red with the operational orbit bump of −3 mm, blue shows the BLM signals with +0.5 mm bump amplitude setting for the experiment. The shift of the loss peak deep into the MB (located from -403.843 m to -418.143 m) is clearly visible. In order to exactly know the luminosity value leading to the quench, the beam separation at IP5 was
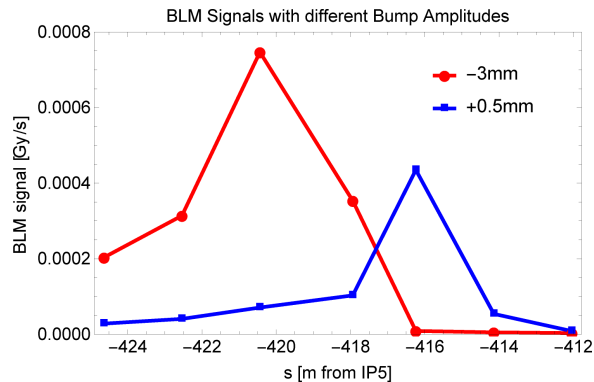
Figure 3: BLM signals for operational (red) and experimental (blue) orbit bump amplitude. The beam is propagating from right to left in this figure.
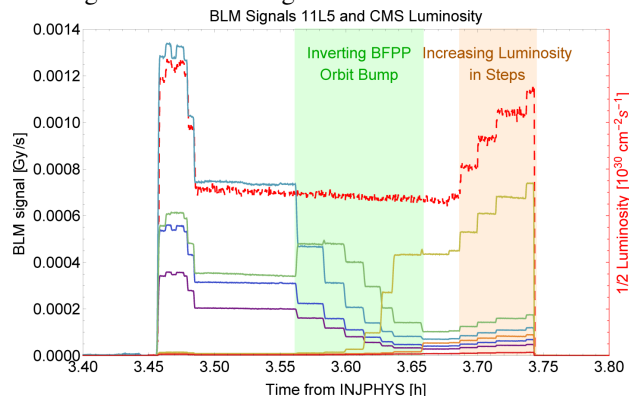

Figure 4: BLM signals and CMS luminosity (red dashed line, divided by 2 to fit the scale) during the quench test.

reduced in steps of 5 μm, waiting a few minutes at each step for conditions to stabilize.

The luminosity in CMS and evolution of the BLM signals around the BFPP impact location during the experiment are shown in Fig. 4. After performing the 4th step and arriving at the head on position, a quench occurred at an instantaneous luminosity of $L \approx 2.3 \times 10^{27}$ cm^{-2}s^{-1} in CMS.

PRELIMINARY ANALYSIS WITH FLUKA

FLUKA shower simulations were carried out to evaluate the peak power density deposited in the magnet coils during the quench test, providing, in turn, a tentative estimate of the steady-state quench level of magnets at $6.37Z$ TeV. To verify the predictive power of the simulation model, simulated BLM signals were compared to measurements. The particle shower simulations were based on BFPP1 loss distributions tracked with MAD-X, assuming an orbit bump of +0.5 mm. As the actual loss location can differ by a few metres from the theoretical one (due to beam screen tolerances etc.), the loss location was adjusted in the FLUKA simulations in order to achieve the best match with the measured BLM signal pattern. This indicated that the actual loss location differed by about $1 − 1.5$ m from the MAD-X prediction for the ideal machine.

Figure 5 compares the measured BLM signals and the simulated ones. In order to demonstrate the sensitivity of the BLM pattern to the impact location of the BFPP1 beam on the beam screen, the figure shows FLUKA results for two different loss locations differing by 50 cm. As can be seen in the plot, such a small shift visibly alters the ratio of BLM signals in the vicinity of the loss location. In general, a very good agreement between simulated and measured signals was achieved for an assumed loss location of 414.8 m left of IP5. Further studies are needed to investigate the potential displacement of the closed orbit and beam pipe with respect to each other, which gives rise to the observed discrepancies between theoretical and actual loss locations.

In order to derive a first estimate of the peak power deposition in the MB coils, a cylindrical mesh was placed over the model of the dipole in FLUKA recording the energy deposited in the magnet coils in volume elements $\Delta z \Delta r \Delta \phi = (10 \, \text{cm}) \times (0.2 \, \text{cm}) \times (2°)$. Figure 6 presents the longitudinal distribution of the peak power density in the MB coils for the simulation with an loss location at 414.8 m left of IP5. Both the peak power density at the inner edge of the cable and the radially averaged density over the cable are shown. Contrary to the BLM pattern, the peak power in the coils is not affected by the position of the loss distribution, because the energy is deposited deep inside the dipole.

As the heat has enough time to spread across the cables' cross-section, one typically uses the radially averaged power density to quantify the quench level for steady-state losses. The maximum radially averaged power density is estimated to be around 15 mW/cm^3, which is lower than previous predictions [13]. As for the BLM pattern, these results should be considered preliminary in view of a subsequent sensitivity analysis. The peak power deposition in the coils depends strongly on the longitudinal and vertical spread of the impact distribution and hence more studies are needed to quantify the uncertainty in the peak power density.

CONCLUSIONS

In the 2015 Pb-Pb run of the LHC, the long-foreseen orbit bumps at loss locations were routinely used to successfully eliminate the quench risk from the BFPP secondary beams. These secondary beams were used to obtain the first accurate measurement of the steady state quench limit of the LHC dipole magnets in an experiment performed on 8 December 2015. The beam of BFPP1 ions created at a luminosity of $L \approx 2.3 \times 10^{27} \, \text{cm}^{-2}\text{s}^{-1}$ quenched a dipole. From previous quench tests, which had never reached the appropriate regime, the steady state quench limit had been inferred to be higher [13]. The detailed analysis of the experiment continues. Nevertheless, it has been shown that the orbit bumps introduced around IP1 and IP5 were essential and will be so in future. The need to install new dispersion suppressor collimators around IP2, to allow the ALICE experiment to operate at the luminosity foreseen in the 2020s, has also been demonstrated.
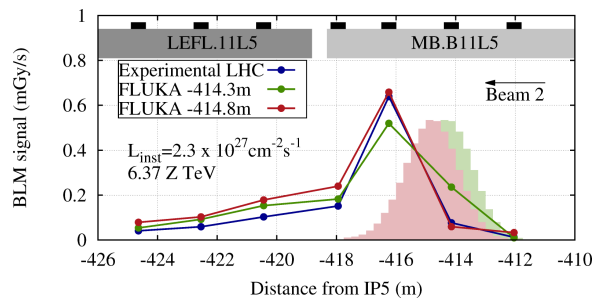
Figure 5: BLM signal comparison between experimental data from the quench test and FLUKA data assuming two different loss locations. The particle distributions for the different loss locations assumed in the simulations are shown in the green and red histograms.
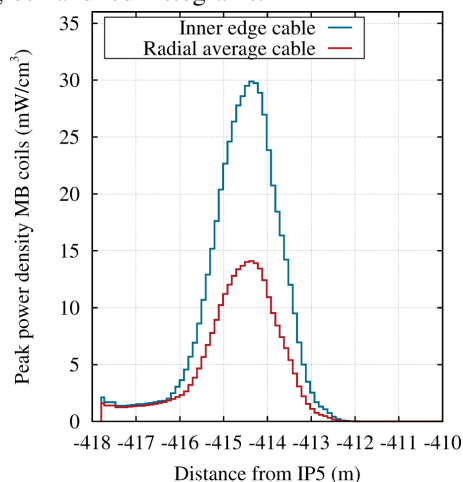

Figure 6: Peak power density in the MB.B11L5 coils during the quench test estimated by FLUKA simulations.

ACKNOWLEDGEMENTS

REFERENCES

[1] S.R. Klein, "Localized beam pipe heating due to e$^-$ capture and nuclear excitation in heavy ion colliders", *Nucl. Instrum. Meth.* **A459**, 51-57 (2001).

[2] J.M. Jowett, J.B. Jeanneret, and K. Schindl, "Heavy ion beams in the LHC" in *Proc. of PAC'03*, Portland, Oregon, TPPB029, p. 1682.

[3] J.M. Jowett, H.H. Braun, M.I. Gresham, E. Mahner, and A.N. Nicholson, "Limits to the performance of the LHC with ion beams", in *Proc. of EPAC'04*, Lucerne, Switzerland, MO-PLT020, pp. 578–580.

[4] R. Bruce, J.M. Jowett, S. Gilardoni, A. Drees, W. Fischer, S. Tepikian, and S.R. Klein, "Observations of beam losses due to bound-free pair production in a heavy-ion collider",in *Phys. Rev. Lett.*, vol. 99, p. 144801, 2007.

[5] R. Bruce, D. Bocian, S. Gilardoni, and J.M. Jowett, "Beam losses from ultraperipheral nuclear collisions between

^{208}Pb^{82+} ions in the Large Hadron Collider and their alleviation", in *Phys. Rev. ST Accel. Beams*, vol. 12, p. 071002, 2009.

[6] M. Schaumann, "Heavy-ion performance of the LHC and future colliders", Ph.D. thesis, III. Phys. Institut, RWTH Aachen University, Aachen, Germany, 2015, urn:nbn:de:hbz:82-rwth-2015-050284, CERN-THESIS-2015-195.

[7] H. Meier *et al.*, "Bound-free electron-positron pair production in relativistic heavy-ion collisions", in *Phys. Rev. A*, vol. 63, p. 032713, 2001.

[8] J.M. Jowett *et al.*, "The 2015 heavy-ion run of the LHC", presented at IPAC'16, Busan, Korea, May 2016, paper TUPMW027, this conference.

[9] C. Bahamonde Castro *et al.*, "Power deposition in LHC magnets due to bound-free pair production in the experimental insertions", presented at IPAC'16, Busan, Korea, May 2016, paper TUPMW006, this conference.

[10] T.T. Böhlen *et al.*, in *Nucl. Data Sheets*, vol. 120, p. 211-214, 2014.

[11] A. Ferrari *et al.*, CERN, Geneva, Switzerland, Rep. CERN-2005-10, 2005.

[12] M. Schaumann *et al.*, "LHC BFPP quench test with ions (2015)", CERN, Geneva, Switzerland, Rep. CERN-ACC-NOTE-2016-0024, `https://cds.cern.ch/record/2127951` (Feb. 2016).

[13] B. Auchmann *et al.*, "Testing beam-induced quench levels of LHC superconducting magnets", *Phys. Rev. ST Accel. Beams*, vol. 18, p. 061002, 2015.